

MORPHOLOGIC MAPPING AND ANALYSIS OF TSIOLKOVSKY CRATER EJECTA. Z. R. Morse¹, G. R. Osinski^{1,2}, and L. L. Tornabene¹ ¹Centre for Planetary Science and Exploration / Dept. of Earth Sciences, University of Western Ontario, 1151 Richmond Street, London Ontario, Canada, N6A 5B7, ²Dept. of Physics and Astronomy, University of Western Ontario, 1151 Richmond Street, London, Ontario, Canada, N6A 3K7 (zmorse@uwo.ca)

Introduction: Tsiolkovsky crater is an elliptical (~200km diameter major axis, by ~180 km diameter minor axis) complex impact structure centered at (129°E, 20°S) on the far side of the Moon. Tsiolkovsky is distinct from other impact craters on the lunar far side due to the presence of a mare deposit overlying much of the crater floor [1], and what has been shown to be an exceptionally rocky surface texture covering parts of the crater rim and ejecta blanket [2]. This structure has been shown to have an age of ~3.2 Ga [2] and is remarkably well preserved due to a lack of subsequent impact cratering in the region.

Here we have used high resolution images and topographic datasets derived from instruments on the Lunar Reconnaissance Orbiter (LRO) to map in detail the locations and extent of various distinct ejecta facies. The type, distribution, and stratigraphic relationships of these ejecta facies provide insight into the formation and emplacement behavior of the Tsiolkovsky ejecta, which in turn provides insight into the formation of other impact structures, the interaction of ejecta with preexisting topography, and their influence on the origin and evolution of planetary crusts.

Methods: We used ~100 m/pixel Lunar Reconnaissance Orbiter Wide Angle Camera (LROC-WAC) images [3] along with elevation data derived from the Lunar Orbiter Laser Altimeter (LOLA) [4], in order to characterize the surface morphology of the Tsiolkovsky ejecta deposits.

Four facies of ejecta were identified based on their morphologies (i.e., texture, relative tonality and structures) as well as documenting their surface area, geographic setting, and stratigraphic relation to one another. Using the Java Mission-planning and Analysis for Remote Sensing (JMARS) program [5], shapefiles were drawn to encompass areas expressing distinct surface morphologies and compiled to form a complete geomorphologic map of the crater and ejecta [Fig. 1].

Results and Facies Descriptions:

Facies A. Facies A extends outward in all directions from the crater rim to radial distances of between ~50km to ~270km. This facies is characterized by a series of groove textures oriented radially to the crater center. Facies A material is observed to overprint preexisting topographic features around Tsiolkovsky. This facies covers a total surface area of ~130,000km².

Facies B. Facies B is identified as distinct chains of similarly sized circular depressions oriented radially from the crater centre. These chains are overlain by

material from Facies A where the two facies coincide, but are not completely infilled by Facies A material. These features become more well-defined the more distant they are from the crater centre, especially beyond the extent of Facies A.

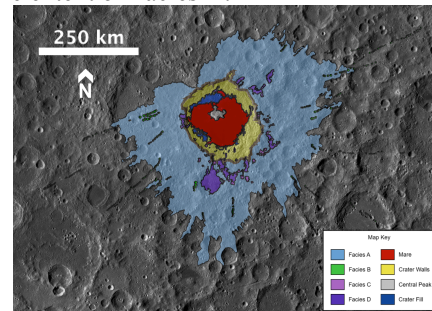


Figure 1 – Morphologic map of Tsiolkovsky crater and ejecta facies. Base image: NASA LRO-WAC Mosaic

Facies C. Facies C consists of relatively flat (i.e., low slopes), smooth surfaced deposits that are constrained within partially to fully enclosed local topographic lows. Deposits of Facies C material can be found both interior to, and exterior to, the crater rim, with a majority of these deposits located ~45–100 km beyond the southeast portion of the crater rim. These deposits overprint portions of Facies A material. Collectively, the units of Facies C materials cover an area of 1,420km².

Facies D. Facies D consists of smooth surfaced units of material that form lobate extensions down local topographic slope into local topographic lows. All observed deposits of Facies D overlie Facies A material. Many Deposits of Facies D are adjacent or connected to deposits of Facies C. The units of Facies C and D appear to be composed of the same material, but the two facies express distinct surface morphologies. Deposits of Facies D material mainly occur to the south and southeast of the crater rim, extending from the topographically high rim to ~95 km across the exterior lunar surface. Some deposits of Facies D material also occur to the northeast of the crater rim extending ~75 km. Collectively, deposits of facies D material cover ~5,400km² of total surface area.

Discussion and Facies Interpretations:

Facies A and B. Based on the above morphologic description and continuous deposition around the crater rim, we interpret Facies A to be the continuous ballistic ejecta blanket of the Tsiolkovsky impact, consisting primarily of melt-poor to –free ballistically em-

placed ejecta material. Similarly, the features of Facies B are interpreted as chains of secondary impact craters due to the distinct radial orientation of the chains and close to overlapping positions of the craters within the chains. These secondary crater chains were formed by relatively large, coherent and high velocity blocks initially ejected by the formation of Tsiolkovsky. These secondary crater chains formed prior to the emplacement of Facies A, as evidenced by the infilling of these secondary craters with ballistic ejecta blanket material where the two facies overlap.

Facies C and D. Due to the smooth-surfaced lobate expressions of both Facies C and D which collectively overprint the radially grooved texture of Facies A, we interpret Facies C and D to be melt-rich ejecta deposits emplaced as a secondary wave of melt-rich material after the deposition of the continuous ballistic ejecta blanket [e.g. 6, 7, 8]. All of the identified melt-rich deposits flow toward or collect in local topographic lows. The deposits of Facies D embay or are emplaced around topographic obstacles. This is consistent with emplacement via a ground-hugging flow that was subject to these topographic constraints [e.g. 6, 7]. The distinct morphologies of Facies C and D are a result of preexisting local topographic conditions. Deposits of Facies C are interpreted to be impact melt ponds as their constituent material settled and collected in enclosed topographic lows. Deposits of Facies D are interpreted to be impact melt flows due to their lobate expression down topographic slopes, extending toward and collecting in local topographic lows.

Facies Distribution. The mapping of all distinct ejecta facies shows several patterns in the overall ejecta emplacement around Tsiolkovsky [Fig. 2]. There is a distinct bilateral symmetry to all ejecta facies along a line running northwest-southeast through the crater center [Fig. 2]. This line of symmetry also describes the major axis of the elliptical crater rim.

The continuous ballistic ejecta blanket (Facies A) is expressed as two distinct lobes that extend perpendicular to this line of symmetry; one to the northeast where the ballistic ejecta extends to the maximum radial distance of ~270 km and one to the southwest where the ejecta blanket reaches a distance of ~200 km from the crater rim (Fig. 2). Conversely, the extent of ballistic ejecta emplacement is shortened parallel to the line of symmetry. Facies A barely extends beyond the crater rim to the northwest, while in the southeast it only extends to a distance of ~100 km from the crater rim.

The melt-rich ejecta facies (Facies C and D) do not display this same two-lobed pattern in their distribution around Tsiolkovsky. Instead there is a notable collection of melt and flow deposits that forms a discontinuous lobate pattern extending from the crater rim and

covering the southeast quadrant. This discontinuous lobate collection of deposits is evenly bisected by the earlier described line of bilateral symmetry. Additionally there are several smaller deposits extending from the crater rim to the northeast and west of the crater center that are also balanced across the line of symmetry (Fig. 2).

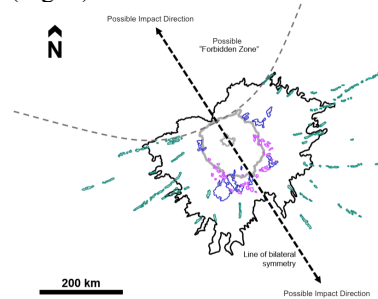


Figure 2 – Sketch of Tsiolkovsky ejecta units illustrating the bilateral distribution of ejecta, potential impact directions, and possible up-range forbidden zone.

Another pattern that emerges from our mapping is a distinct lack of continuous ballistic ejecta (Facies A) and secondary crater chains (Facies B) to the northwest of the crater. We present two hypotheses for this lack of ballistic ejecta deposits: 1) The lack of secondary craters and truncated ballistic ejecta blanket are both consistent with a “Forbidden Zone” where, in low angle impacts, ballistic ejecta emplacement is limited in the up-range direction [9]. 2) The presence of a pre-existing topographic high to the northwest of the crater may have shielded the surrounding region from overprinting by Tsiolkovsky ejecta.

Conclusions: A line of symmetry in ejecta deposits has been shown to parallel the impact direction at other lunar impact structures (e.g., [7]). Thus, the impact direction for the Tsiolkovsky-forming impact can be constrained to either the northwest or southeast. Additional evidence for this interpretation of the impact direction comes from the observed collinear ellipticity of the crater planform. The impact direction for Tsiolkovsky could be further constrained by confirming the presence of a forbidden zone to the northwest.

References: [1] Guest J.E., & Murray J.B. (1969) *Plan. and Space Sci.* 17, 121-141. [2] Greenhagen et al. (2016) *Icarus* 273, 237-247. [3] Robinson et al. (2010) *Space Sci. Rev.* 150, 81-124. [4] Chin et al. (2007) *Space Sci. Rev.* 129, 391-419. [5] Christensen P. R. et al. (2009) *AGM, Fall Meeting*. Abstract IN22A-06. [6] Neish et al. (2014) *Icarus* 239, 105-117. [7] Morse et al. (2018) *Icarus* 299, 253-271. [8] Osinski et al. (2011) *Earth and Plan. Sci. Let.* 310, 167-181. [9] Herrik R. R. & Frosberg-Taylor N. K. (2003). *Meteorit. Plan. Sci.* 38, 1551-1578